



**Structure-performance correlations of cross-linked boronic acid polymers as adsorbents for recovery of fructose from glucose-fructose mixtures**

Journal:	<i>Green Chemistry</i>
Manuscript ID	GC-ART-09-2019-003151.R1
Article Type:	Paper
Date Submitted by the Author:	08-Dec-2019
Complete List of Authors:	Schroer, Guido; RWTH Aachen University Deischer, Jeff; RWTH Aachen, Institut für Technische und Makromolekulare Chemie Zensen, Tobias; RWTH Aachen University Kraus, Jan; University of Würzburg Poppler, Ann-Christin; University of Würzburg, Organic Chemistry Qi, Long; Ames Laboratory, Division of Chemical & Biological Sciences Scott, Susannah; University of California, SB, Chemical Engineering Delidovich, Irina; RWTH Aachen University,



Journal Name

ARTICLE

# Structure-performance correlations of cross-linked boronic acid polymers as adsorbents for recovery of fructose from glucose-fructose mixtures

Received 00th January 20xx,  
Accepted 00th January 20xx

DOI: 10.1039/x0xx00000x

www.rsc.org/

Guido Schroer,<sup>a</sup> Jeff Deischer,<sup>a</sup> Tobias Zensen,<sup>a</sup> Jan Kraus,<sup>b</sup> Ann-Christin Pöppler,<sup>b</sup> Long Qi,<sup>c</sup> Susannah Scott,<sup>d,e</sup> and Irina Delidovich<sup>a,\*</sup>

Recovery of bio-oxygenates from the reaction mixtures is one of the major challenges for future bio-refineries. Isolation of fructose produced by isomerization of glucose presents a typical example at a very early stage of the value chain. We propose to recover fructose from a solution containing a mixture of glucose and fructose by adsorption on polymers bearing phenylboronate moieties. *p*-vinylphenylboronic acid was polymerized with various cross-linkers, namely polar aliphatic, low-polarity aliphatic, and aromatic. The cross-linker content was in the range 5-40 mol%. The polymers exhibit high capacities for fructose, with a maximum loading of up to 1 mol<sub>Fruc</sub> mol<sub>B</sub><sup>-1</sup>. Fructose loading depends significantly on the length and content of cross-linker, as well as pre-treatment of the polymer. In general, the maximum fructose capacity correlates with the swelling ability of the polymers, since phenylboronate moieties become available for adsorption upon swelling. In contrast, maximum glucose loadings are much lower, in the range 0.1-0.3 mol<sub>Glu</sub> mol<sub>B</sub><sup>-1</sup>, and depend only slightly on the type of cross-linker. The structures of the glucose and fructose complexes and the kinetics of their uptake were studied by *in situ* MAS NMR. Efficient desorption of fructose was observed in acidic medium, and more importantly, using CO<sub>2</sub>. The structures of the polymers after repeated adsorption and desorption remain unchanged, as confirmed by solid-state NMR. Adsorption-assisted isomerization of glucose catalyzed by soluble carbonates was also studied. A 56% yield of fructose was achieved after 8 successive cycles of reaction and adsorption.

## Introduction

Carbohydrates are major compounds obtained from biomass valorisation. They are frequently discussed as key intermediates for the production of renewable fuels as well as bulk and fine chemicals in future bio-refineries.<sup>1, 2</sup> Glucose, as

a primary product, is readily available from cellulose *via* hydrolysis.<sup>3</sup> Fructose is obtained from glucose by isomerization.<sup>4, 5</sup> Importantly, the isomerization is an equilibrium reaction with  $K_{eq} \approx 1$  at 50 °C.<sup>6, 7</sup> Fructose is considered a more valuable product, as it can be selectively converted to promising bio-based platform chemicals, such as 5-HMF<sup>8</sup> and levulinic acid.<sup>9, 10</sup> Aside from its relevance for bio-refineries, the isomerization reaction is of further industrial importance. Glucose-fructose syrups are widely used as sweeteners. Due to the higher sweetening power of fructose compared to glucose, high fructose contents are desired. Glucose-fructose syrups are currently manufactured by enzymatic isomerization, followed by a separation process. Fructose concentrations of 42 mol% after isomerization can be increased to 90 mol% by chromatographic procedures such as

*a* - Chair of Heterogeneous Catalysis and Chemical Technology, RWTH Aachen University, Worringerweg 2, 52074 Aachen, Germany, e-mail: delidovich@itmc.rwth-aachen.de

*b* - Institute of Organic Chemistry, University of Würzburg, Am Hubland, 97074 Würzburg, Germany

*c* - U.S. DOE Ames Laboratory, Iowa State University, Ames, Iowa 50011, United States

*d* - Department of Chemistry & Biochemistry, University of California, Santa Barbara, California 93106, United States.

*e* - Department of Chemical Engineering, University of California, Santa Barbara, California 93106, United States. Electronic Supplementary Information (ESI) available: [details of any supplementary information available should be included here]. See DOI: 10.1039/x0xx00000x

simulated moving bed chromatography.<sup>11</sup> Developing a more facile method for fructose synthesis would promote its industrial use in value chains for production of fuels or commodities. In this regard, chemo-catalytic processes, which are typically less expensive than enzymatic processes, associated with a suitable technique for separation of the product, are highly desirable. Significant efforts have been made to design suitable chemo-catalysts for the glucose-fructose isomerization.<sup>4, 12</sup> At the same time, developing facile and energy-efficient techniques for fructose isolation represents a challenge. Conventional separation techniques, such as distillation, cannot be used to isolate fructose since the compound is highly polar and non-volatile.<sup>13</sup>

One method to separate glucose and fructose is based on their reversible esterification as boronates. The latter form cyclic esters with molecules bearing a 1,2-diol motif, such as saccharides.<sup>14</sup> The affinity of a saccharide for the boronate depends on the saccharide structure.<sup>15-17</sup> Fructose typically exhibits much higher complexation constants with boronates than glucose. With phenylboronates the association constants are  $K = 110$  for glucose and  $K = 4370$  for fructose, respectively.<sup>18</sup> This phenomenon is called “molecular recognition”: boronates “recognize” fructose in the presence of glucose and selectively build a complex with the former.<sup>19</sup> Several analytical methods have been designed based on molecular recognition, including boronate affinity chromatography<sup>20</sup> and boronate affinity saccharide electrophoresis.<sup>21</sup> Recently, a number of preparative methods were proposed based on molecular recognition with boronates for recovery of saccharides, diols, and polyols produced from biomass.<sup>22-34</sup> A few studies were aimed at fructose isolation. Typically, these approaches are based on the extraction of a fructose-boronate anionic complex into an organic phase, while glucose remains in the aqueous phase.<sup>29, 35-38</sup> However, some challenges connected with the extraction process remain unsolved. These include the necessity of using an organic solvent as well as the need for environmentally unfriendly quaternary amines as counter-cations for the fructose-boronate anionic complex in the organic phase. Leaching of boron into the aqueous phase presents another challenge. These disadvantages of liquid-liquid anionic extraction may be overcome by implementing an adsorption-based separation process using polymers bearing boronate functionalities. Barker et al. proposed the idea of adsorption-assisted glucose isomerization to fructose for the first time in the 1970s.<sup>39</sup> They used a *p*-vinylphenylboronic acid (*p*-VPBA) polymer cross-linked with ca. 5% divinylbenzene (DVB) for *in situ* adsorption of fructose upon isomerization of glucose in the presence of NaOH. This enabled isolation of adsorbed fructose and an increase in fructose yield up to 57 % was reported. The process was emphasized as promising and future studies proclaimed, but research ceased without further reasoning.

In this study, we revisit the previously proposed approach, aiming to elucidate relationships between the molecular structure of the polymers and their adsorption capacities. Fig. 1 schematically represents the steps undertaken. First, the polymers were synthesized with various types and contents of

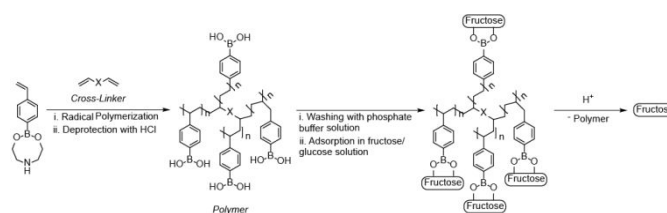


Figure 1 Schematic representation of the proposed separation of fructose using adsorption on boron-containing polymers. Structures of cross-linkers are provided in Tab. 1.

cross-linkers. Adsorption of fructose and glucose on the polymers, as well as their subsequent desorption, were studied. To obtain molecular-level insight on the structure-performance relationships, significant effort was expended in material characterization including classical solid-state NMR and *in situ* monitoring of adsorption by MAS-NMR. Finally, adsorption-assisted isomerization of glucose to fructose was performed in the presence of carbonate buffer ( $\text{Na}_2\text{CO}_3 + \text{NaHCO}_3$ , pH 10) as catalyst.

## Experimental

### Chemicals

Unless specified, all chemicals were used without further purification. *p*-Vinylphenylboronic acid (*p*-VPBA, 97%) was supplied by ChemPUR. D-(-)-fructose (Ph.Eur.), 1,4-phenylene dimethacrylate (PDMA; >99%) and 2,2'-azobis(2-methylpropionitrile) (AIBN, >98%) were purchased from Sigma-Aldrich. D-(+)-glucose (Reag. Ph. Eur.) and sodium dihydrogen phosphate monohydrate (Reag. Ph. Eur.) were provided by Merck. Sodium hydrogen carbonate (>99%) and chloroform (>99%) from Roth and conc. hydrochloric acid (37wt%) from Honeywell were used. Toluene (>99.7%), sulfuric acid (98%), ethanol (99.9%), anhydrous benzyl alcohol (>99.8%) and sodium hydroxide microgranulate ( $\geq 98.8\%$ ) were obtained from GeyerChemSolute. Divinyl sulfone stabilized with 0.05% hydroquinone (DVS, 97%), ethylene glycol dimethacrylate stabilized with 100 ppm mehq (EDMA, 98%), triethylene glycol dimethacrylate stabilized with 200-300 ppm mehq (TDMA; 95%), 1,7-octadiene (OD; 98%), 1,9-decadiene (DD, 98%) and 1,13-tetradecadiene (TD, 90+%) were purchased from Th. Geyer. Diethanolamine (DEA, 99%) and divinylbenzene (DVB, 80% divinylbenzene: 20% ethylbenzene mixture, 99%) were provided by Alfa Aesar. All solutions were prepared in distilled water.

### Esterification of *p*-VPBA

The esterification method described in the literature was optimized.<sup>40</sup> In a typical procedure, stoichiometric amounts of *p*-VPBA (16.00 g, 108 mmol) and DEA (11.36 g, 10.36 mL, 108 mmol) were added to 640 mL toluene used as an azeotropic solvent. The reaction mixture was heated to 115 °C and water was successively removed with a water separator. After 2 h, the reaction mixture was cooled in an ice bath and the cold solution filtered over a glass frit. The recovered iminodiethyl *p*-vinylphenylboronate was extensively washed with toluene, dried under high vacuum, and stored in a freezer. The product was obtained as a white powder in yields

ranging from 80-95%. The structure was confirmed by  $^1\text{H}$ - and  $^{13}\text{C}$ -NMR. Spectra are provided in Supplementary Information (Fig. 1S-2S).

### Synthesis of 2,6-Divinyl-naphthalene

2,6-divinyl-naphthalene is the only cross-linker that was not commercially available. Its synthesis is based on a literature procedure.<sup>41</sup> 2,6-Dibromonaphthalene (2.63 g, 9.20 mmol), potassium vinyltrifluoroborate (3.7 g, 27.62 mmol),  $\text{PdCl}_2$  (0.10 g, 0.55 mmol),  $\text{Cs}_2\text{CO}_3$  (18.0 g, 55 mmol) and  $\text{PPh}_3$  (0.43 g, 1.64 mmol) were dissolved in 50 mL of a 9:1 v:v mixture of degassed THF and water. The solution was refluxed at 75 °C under a nitrogen atmosphere for 16 h. After cooling to RT, the solvent was removed under reduced pressure. Water (75 mL) was added to the residue and the aqueous phase was extracted with ethyl acetate (3 x 20 mL). The combined organic extracts were then successively washed with 50 mL water and 25 mL brine, dried over  $\text{MgSO}_4$ , and the solvent removed under reduced pressure. After column chromatography with neat *n*-heptane and solvent removal under reduced pressure, the product was obtained as a white solid (1.18 g, 71%). The structure was confirmed by NMR (Fig. 3S).

### Synthesis of cross-linked *p*-VPBA Polymers

Polymerization was based on a previously reported procedure.<sup>39</sup> Iminodiethyl *p*-vinylphenylboronate (5.00 g, 23.03 mmol) and AIBN (14 mg, 0.4 mol%) were dissolved in 14 mL dried and degassed benzyl alcohol. Varying amounts and types of cross-linker were added (Tab. 1S, SI). The mixture was degassed in a 50 mL Schlenk-flask for 30 min. The reaction was allowed to proceed under an Ar atmosphere for 20 h at 80 °C. The solid product was ground, washed with chloroform, dried on a glass frit, and stored in a vacuum desiccator (60 °C). After drying, the product was finely ground with a mortar and pestle, washed three times successively with 70 mL aqueous 1 M hydrochloric acid solution, water, and a 0.5 M aqueous phosphate buffer solution (pH 7.5, prepared by dropwise addition of 4 M NaOH to 0.5 M aqueous  $\text{NaH}_2\text{PO}_4$  until pH 7.5 was reached). The product was obtained as a white powder after drying in a vacuum desiccator at 60 °C. Polymer yields ranged from 62% (not cross-linked) to 99% (Tab. 1S).

### Buffer Solutions

Two types of buffer solutions were used in this study, namely, a phosphate and a carbonate buffer. The carbonate buffer solution was obtained by mixing of 0.5 M aqueous carbonate buffer ( $\text{Na}_2\text{CO}_3$  +  $\text{NaHCO}_3$ , pH 10, prepared by dropwise addition of 4 M NaOH to 0.5 M aqueous  $\text{NaHCO}_3$  until pH 10 was reached) with ethanol in a ratio 80:20 v:v. The phosphate buffer solution was obtained by mixing of 0.5 M aqueous phosphate buffer ( $\text{Na}_2\text{HPO}_4$  +  $\text{NaH}_2\text{PO}_4$ , pH 7.5, prepared by dropwise addition of 4 M NaOH to 0.5 M  $\text{NaH}_2\text{PO}_4$  until pH 7.5 was reached) with ethanol in a ratio 80:20 v:v.

### Adsorption Isotherms

Stock solutions for recording adsorption isotherms were prepared by dissolving 0.063 - 1.250 g of either glucose or

fructose in 18.75 mL carbonate buffer solution. Each stock solution (2.63 mL) was added to 0.100 g polymer and the resulting solution was stirred at 500 rpm for 3 h at room temperature (RT). The solutions were filtered with polyamide syringe filters (Chromafil PA 20/25) and analysed by HPLC.

For competitive sorption studies, stock solutions were prepared in the same manner, using a 70:30 mol%:mol% mixture of glucose and fructose.

### Desorption and Recycling

After adsorption, each polymer was filtered over a glass frit and dried under high vacuum. Different acid solutions were screened for desorption (Tab. 5). In a typical procedure, the desorption solution (2.63 mL) was added to 0.100 g polymer containing adsorbed fructose, and the solution was allowed to stir for 4 h at 500 rpm. The solutions were processed and analysed by HPLC as described above.

For polymer recycling, each polymer was filtered over a glass frit, dried under high vacuum, and used in a second adsorption-desorption cycle.

### Adsorption-Assisted Isomerization

A 50 mL two-necked round-bottom flask was charged with 1 g glucose and 9 mL carbonate buffer (resulting in a 10 wt% glucose solution). Isomerization was allowed to proceed for 1 h at 63 °C. These reaction conditions were chosen based on previous screening studies (Fig. 32S-35S). After the reaction, the solution was cooled quickly using an ice bath and once RT was reached, 6.57 mL solution was added to 0.250 g polymer. The resulting mixture was stirred at 500 rpm for 3 h at RT. The solution was filtered with a polyamide syringe filter (Chromafil PA 20/25) to remove the polymer. To restore the initial sugar concentration, 4 mL of the filtrate was combined with 6 mL of a fresh 10.5 wt% glucose solution for use in the next isomerization step. Eight consecutive adsorption-separation cycles were performed. 1 mL aliquots of the solution prior to isomerization, after isomerization and after adsorption were analysed by HPLC.

### Solid-State NMR

All solid-state NMR experiments were performed with unlabelled material on a Bruker Avance III NMR Spectrometer at 14.1 T with either 20 or 24 kHz MAS. A 3.2 mm HX probe was used. In all cases, the  $^1\text{H}$  90° pulse duration was 2.5  $\mu\text{s}$ . For  $^1\text{H}$ - $^{13}\text{C}$  cross-polarization (CP) experiments, a 2 ms contact time with a ramp on the  $^1\text{H}$  channel was used. During acquisition, SPINAL64 heteronuclear decoupling was employed.  $^1\text{H}$ - $^{13}\text{C}$  CP FSLG-HETCOR experiments were recorded using the same setup, but with shorter and varying contact times. Chemical shifts were referenced using adamantane.  $^{11}\text{B}$  NMR spectra were acquired using the Hahn-echo sequence to reduce the background signal from the probe. All experiments were nominally performed at RT. However, frictional heating due to MAS results in a higher actual sample temperature. Spectral processing was done using the Bruker TopSpin 3.5 software. In particular, FIDs in  $^{11}\text{B}$  Hahn-echo experiments were left-shifted to the echo maxima.

**In-Situ MAS <sup>13</sup>C-NMR**

The kinetics of carbohydrate sorption were measured on an Avance IPSO 500MHz WB NMR Spectrometer (11.7 T) equipped with an MAS double resonance broadband <sup>1</sup>H/X probe. The 4-mm NMR rotor was loaded with 4 mg of either 1-<sup>13</sup>C-glucose or 2-<sup>13</sup>C-fructose (22 μmol), 6 mg of 20 mol% DVB-cross-linked polymer and 75 μL of an 80:20 mixture (v:v) of 0.5 M NaHCO<sub>3</sub> buffer in D<sub>2</sub>O (pH adjusted to 10 with 4 M NaOH) and EtOH. Time-dependent <sup>13</sup>C direct polarization spectra without <sup>1</sup>H decoupling were recorded at an MAS rate of 5 kHz. Each spectrum acquisition required 20 min, for a total experiment time of 4 h.

**Elemental Analysis**

Elemental analysis was performed using an ICP-OES Spectroblue Instrument from Spectro Analytical Instruments. 20-30 mg sample, 1 g KOH and 0.12 g KNO<sub>3</sub> were fused in a china jar. The melt cake was added to 50 mL aqueous 10 wt% hydrochloric acid solution and analyzed. Carbon, hydrogen and nitrogen contents were measured with a 2400 Series II CHNS/O Elemental Analyzer from Perkin Elmer. Blank samples and acetanilide as standard were used for instrument calibration. Selected samples of polymers were analyzed in Mikroanalytisches Laboratorium Kolbe in Mülheim.

**Nitrogen and Water Vapor Physisorption**

Nitrogen adsorption/desorption isotherms were recorded on a Quadrasorb SI instrument from Quantachrome/3P Instruments. Prior to the measurement, the sample was degassed at 60 °C for 16 h. Total pore volume was monitored at relative pressures of 0.900 *p/p*<sub>0</sub>. Water vapour adsorption was measured at 20 °C on an Autosorb iQ instrument from Quantachrome/3P Instruments. Before the measurement, the sample was degassed at 60 °C until it passed the degassing test (21 mTorr min<sup>-1</sup>). Pore volume was calculated at relative pressures of 0.900 *p/p*<sub>0</sub> after an equilibration time of 5 min.

**Swelling Degree**

Polymer swelling was assessed gravimetrically, according to a literature procedure.<sup>42</sup> 0.100 g polymer was placed in a 5 mL centrifuge tube inlay. The weights of the empty (*m*<sub>1</sub>) and filled (*m*<sub>2</sub>) inlays were noted. The filled inlay was inserted into a 15 mL centrifuge tube and the tube was filled with the specified soaking solution. Swelling was monitored in the carbonate buffer. For the determination of the swelling degrees in presence of glucose and fructose, 0.500 g of the respective sugar were added to the solution and samples ultrasonically mixed for 3 h. HPLC samples were taken prior and after the procedure to determine and subtract the adsorbed amounts of glucose and fructose from *m*<sub>3</sub>. After standing for 24 h, the supernatant liquid was removed, and the tube was centrifuged for 15 min at 4000 rpm. The inlay was recovered and its weight (*m*<sub>3</sub>) noted. The swelling degree *SD* was determined using equation 1.

$$SD = \frac{(m_3 - m_1) - (m_2 - m_1)}{m_2 - m_1} \cdot 100\% \quad (\text{Eq.1})$$

**Determination of the Cross-linker Length**

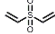
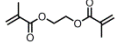
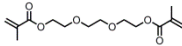
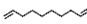

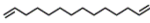
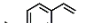
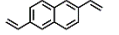
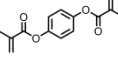
Molecular structures were geometry optimized using the MM2 method. First, the rigid molecule was placed in a cylinder with a minimum diameter. The center of gravity of the molecule was initially located in the centroid of the cylinder. The optimization function rotates the molecule in space until the maximum squared radius is minimized. Since the cylinder fit is rotationally symmetric, the function takes only the *x* and *y* coordinates into account to reduce the number of variables. Thus, the optimization is reduced to a 2D solver problem. The function was solved using the Matlab® globalSearch function from the Global optimization toolbox.<sup>43</sup> An additional optimization was performed to translate the molecule into cylindrical form to further reduce the cylinder radius.

**HPLC**

The concentrations of fructose and glucose were determined by high performance liquid chromatography (HPLC) using a Shimadzu Prominence LC-20 system. Samples containing only fructose or glucose were injected into two successively connected organic acid resin columns (CS-Chromatography, 100 × 8.0 mm and 300 × 8.0 mm) connected *via* a 6-port switching valve equipped with two pumps (A + B). The columns were heated to 40 °C and the eluent (154 μL CF<sub>3</sub>COOH in 1 L of water) was supplied at a flow rate of 1 mL min<sup>-1</sup>. During the first 7 min after injection, the eluent was supplied with pump A and flowed through the connected columns as well as a refractive index (RI) detector. Then, the valve position was switched to allow elution through each column separately for the next 18 min. Using pump A, the eluent was pumped through the first column (100 × 8.0 mm), and a photodiode array (PDA) detector with a detection wavelength of 270 nm, to analyse possible furanic by-products. Simultaneously, the eluent was pumped through a second column (300 mm × 8.0 mm) and the RI detector using pump B, to analyse monosaccharides and acidic by-products.

Samples containing both glucose and fructose were first diluted by factor of 10 prior to analysis. 10 mL of each diluted sample was treated successively with 200 mg of Amberlyst® 15 for 30 min, and 500 mg ion-exchange resin Amberlyte® IRA-96 free base for 1 h each. Samples were injected into a Phenomenex 5 μL Luna-NH<sub>2</sub> column (250 × 4.6 mm) and eluted at 35 °C with an eluent (acetonitrile and water in a ratio 80:20 v:v) supplied at a rate of 1 mL min<sup>-1</sup>. The system was equipped with an RI detector. An example chromatogram and the corresponding calibration curves are provided in the SI (Fig. 4S). An HPLC error of 2% was estimated for determination of glucose and fructose concentrations. Selected adsorption experiments were performed in duplicate or triplicate.

Table 1: Composition and properties of synthesized polymers, SD stands for swelling degree.

Entry	Name	Cross-Linker Structure	Length [Å]	Amount [mol%]	Boronic Acid Content		Pore Volume		SD [%]
					Calc.	Found	N <sub>2</sub>	H <sub>2</sub> O	
1	Not cross-linked		-	0	6.733	4.672 (69%)			107
2	Divinylsulfone (DVS)		9.6	20	5.617	4.117 (73%)	0.004	0.23	67
3	Ethylene glycol dimethacrylate (EDMA)		14.9	5	6.275	4.080 (65%)	0.004	0.20	74
4				20	5.212	3.663 (70%)			60
5				40	4.252	2.895 (68%)			45
6	Triethylene glycol dimethacrylate (TDMA)		22.0	20	4.725	3.441 (73%)	0.002	0.24	56
7	1,7-octadiene (OD)		13.0	20	5.668	4.330 (76%)	0.005	0.26	77
8	1,9-decadiene (DD)		15.5	20	5.493	4.791 (87%)	0.006	0.25	80
9	1,13-tetradecadiene (TD)		20.6	20	5.062	4.293 (85%)	0.006	0.26	85
10	Divinylbenzene (DVB)		11.9	5	6.353	3.996 (63%)	0.005	0.22	75
11				20	5.432	3.506 (65%)			68
12				40	4.552	3.219 (71%)			46
13				20	5.252	3.717 (71%)			70
14	2,6-divinyl naphthalene (DVN)		13.6	20	5.252	3.717 (71%)	0.002	0.21	70
14	1,4-phenylene dimethacrylate (PDMA)		15.1	20	4.911	3.219 (66%)	0.006	0.23	71

## Results and Discussion

### Polymer Synthesis and Characterization

Polymers with different cross-linkers were synthesized as shown in Fig. 1. *p*-vinylphenylboronic acid was protected with DEA and co-polymerized with the respective cross-linker. A high boron content is a prerequisite for high sorption capacity, since adsorption takes place by stoichiometric esterification. Therefore, the cross-linker content was kept low, in the range of 5 to 40 mol%. The types of cross-linkers used are listed in Tab. 1. They include polar aliphatic (DVS, EDMA, and TDMA), low-polarity aliphatic (OD, DD, and TD), and aromatic (DVB, DVN, and PDMA) molecules. The cross-linkers differ in length, as estimated by the cylinder fitting procedure. The polymers were obtained in high yields of 62-99%. The boron contents range from 60 to 90% of the theoretical amounts (Tab. 2S-3S). Loss of boron moieties can be explained by partial hydrolysis during synthesis. In addition, IR spectra of polymers containing EDMA, TDMA and PDMA exhibit a characteristic carbonyl stretching band at ca. 1700 cm<sup>-1</sup>. As expected, this band is absent in the spectra of other polymers (Fig. 5S-7S). The dry polymers are non-porous, as shown by nitrogen physisorption (Tab. 1). Estimated specific surface areas of the polymers were ca. 1 m<sup>2</sup> g<sup>-1</sup>. However, pore volumes of all materials are significantly higher as determined in physisorption with water than nitrogen, indicating that the polymers swell in aqueous solution. Hence, the swelling was studied by gravimetric analysis in the carbonate buffer, particularly because the same buffer was later used for the adsorption isotherm experiments

as well as during the adsorption-assisted isomerization of glucose into fructose. Swelling degrees determined for all synthesized polymers are listed in Tab. 1. The content of cross-linker was varied for EDMA and DVB. In both cases, the swelling degree decreases upon increasing the cross-linker amount. The swelling degree can be further correlated with the length of the cross-linker: for low-polarity aliphatic (entries 7-9, Tab. 1) and aromatic (entries 11, 12, 14, Tab. 1) cross-linkers, longer cross-linkers result in higher swelling degrees. Unexpectedly, the swelling degree of polymers containing highly polar cross-linkers decreases as the length of the cross-linker increases (entries 2, 4, and 6, Tab. 1). This effect is probably associated with the higher oxygen content of the longer cross-linkers, leading to a change in interaction with components of the solvent (i.e., water and ethanol). Thus, highly polar cross-linkers are most probably solvated by water, whereas low-polarity cross-linkers are solvated by ethanol. Apparently, these solvation differences reflect an inverse dependence of the swelling degree on the length for highly polar cross-linkers. The polymers were further characterized by <sup>1</sup>H, <sup>13</sup>C and <sup>11</sup>B MAS NMR. For the cross-linked polymers, linker-specific resonances were present in addition to resonances observed for the uncross-linked polymer. To facilitate assignments, the solution-state spectrum of the uncross-linked polymer was recorded in a mixture of THF-*d*<sub>6</sub> and D<sub>2</sub>O (9:1 v:v). The resonances for the dissolved polymer generally appeared at the same chemical shifts as for the solid sample (Fig. 8S), but the solution-state resonances were much narrower than the solid-state resonances. Using this information in combination with literature data on polystyrene, all polymer signals were assigned.<sup>44</sup> An atactic

structure was deduced from the distribution of  $^{13}\text{C}$  chemical shifts around 40 - 50 ppm corresponding to the  $\text{CH}_2$  group of the backbone in both the solid state and in solution. In addition to the characteristic polymer signals, resonances were observed at 52 and 62 ppm. They are assigned to DEA, used as the protecting agent, although the nitrogen content is below the detection limit of the CHN analysis. Moreover, the polymer contains residual benzyl alcohol used as the solvent for polymerization, based on the presence of a  $^{13}\text{C}$  resonance at 64 ppm as well as a signal at 4.5 ppm in the  $^1\text{H}$  NMR spectrum.  $^1\text{H}$ - $^{13}\text{C}$  HETCOR MAS NMR experiments (Fig. 9S) confirm these assignments.

In addition to the general  $^1\text{H}$  and  $^{13}\text{C}$  NMR characterization of the polymers (Fig. 10S), the nature of the boron functionality is important for their desired application as fructose recovery materials. Two characteristic broad signals at 15-30 ppm and 0-10 ppm corresponding to  $\text{sp}^2$ - and  $\text{sp}^3$ -hybridized boron, respectively, were observed in the  $^{11}\text{B}$  MAS NMR spectra (Fig. 11S).<sup>45</sup>

### Adsorption Isotherms

After characterization, the polymers were tested for fructose and glucose sorption. First, the sorption conditions were screened and optimized using a polymer cross-linked with 20 mol% DVB. Addition of an organic solvent to the aqueous buffer solution was necessary to ensure polymer dispersion since the polymers are not wetted in pure aqueous solution. Different organic co-solvents were tested to improve the wettability of the polymers (Tab. 4S). The best results were achieved by adding 20 vol% ethanol to the aqueous sugar-buffer solution. Sorption experiments were performed in both a carbonate buffer solution (pH 7.5 and pH 10) and a phosphate buffer solution (pH 7.5 and pH 10). Significantly lower sugar adsorption was noted at pH 7.5, which can be explained by its lower pH. A greater fraction of boron is  $\text{sp}^3$ -hybridized at pH 10 than at pH 7.5.<sup>46</sup> In addition, performing the sorption at pH 10 in the phosphate buffer a significant decrease of the pH during the adsorption is noted, as the pH is above the buffer regime of the buffer system.<sup>47</sup> Sorption isotherms were therefore recorded in the carbonate buffer solution (pH 10) to which 20 vol% EtOH was added

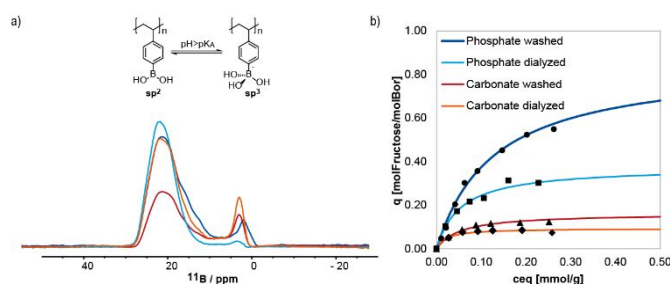


Figure 2: a)  $^{11}\text{B}$  MAS-NMR spectra of polymers cross-linked with 20 mol% DVB recorded with the Hahn-echo-sequence after various pre-treatments, b) fructose sorption isotherms of the variously pre-treated and dialysed polymers. Conditions: 0.100 g polymer, 2.63 mL carbonate buffer solution, 0.063 -1.250 g fructose, 3 h, RT.

(Tab. 5S). The sorption equilibrium was reached after approximately 3 h for fructose, and 90 min for glucose (Fig. 12S and 13S). The Langmuir model was used to analyse the measured adsorption isotherms. Importantly, the glucose adsorption isotherms are saturation curves, whereas saturation was not typically obtained for fructose sorption. Thus, the maximum fructose capacity was deduced using the best fit of the Langmuir isotherm equation. In addition, 4-bromopolystyrene cross-linked with 20% DVB was tested for sugar sorption under optimized conditions. No sorption was found, confirming the necessity of boronate moieties for sugar sorption. After optimization, the influence of the polymer pre-treatment on the sorption behaviour was studied. The synthetic procedure includes the polymerization of *p*-vinylphenylboronic acid protected with DEA, followed by washing with HCl to remove the protecting group (Fig. 1). The resulting polymers contain mainly boronic acid groups in  $\text{sp}^2$  hybridization, whereas a  $\text{sp}^3$  hybridization of the boronic acid ("boronate") is more favourable for complexation.<sup>33, 46</sup> For anionic extraction of saccharides, the boron-containing species were treated with a basic solution to convert the boronic acid sites into boronates to facilitate sorption.<sup>35</sup> In this study, we washed the polymers with either a phosphate buffer (pH 7.5) or a carbonate buffer (pH 10.0) and dried them afterwards. Subsequently, the washed polymers were purified by dialysis against water. Fig. 2a compares the  $^{11}\text{B}$  MAS NMR spectra of polymers after the washing pre-treatments and dialysis.

Table 2: Maximum fructose and glucose sorption capacities for the polymers with various content of DVB and EDMA cross-linkers, based on Langmuir isotherm fits.

Entry	Cross-Linker	Fructose		Glucose	
		$\text{mol}_{\text{Fru}}\text{mol}_{\text{B}}^{-1}$	$\text{mmol}_{\text{Fru}}\text{g}^{-1}$	$\text{mol}_{\text{Glu}}\text{mol}_{\text{B}}^{-1}$	$\text{mmol}_{\text{Glu}}\text{g}^{-1}$
1	DVB, 5%mol%	1.478	5.906	0.266	1.064
2	DVB, 20mol%	0.854	2.993	0.201	0.704
3	DVB, 40mol%	0.499	1.607	0.139	0.477
4	EDMA, 5mol%	1.108	4.519	0.206	0.840
5	EDMA, 20mol%	0.618	2.261	0.171	0.627
6	EDMA, 40mol%	0.344	0.997	0.111	0.322

Conditions: 0.100 g polymer, 2.63 mL carbonate buffer solution, 0.063 -1.250 g fructose or glucose, 3 h, RT. \* - fit based on adsorption at low concentrations, since the highly viscous solution became impossible to filter at high concentrations.

Table 3 : Maximum fructose and glucose sorption capacities based on a Langmuir isotherm fit for polymers cross-linked with 20 mol% of different cross-linkers.

Entry	Cross-Linker	Fructose		Glucose	
		mol <sub>Fructose</sub> mol <sub>B</sub> <sup>-1</sup>	mmol <sub>Fructose</sub> g <sup>-1</sup>	mol <sub>Glucose</sub> mol <sub>B</sub> <sup>-1</sup>	mmol <sub>Glucose</sub> g <sup>-1</sup>
1	DVS, 20mol%	0.294*	1.652*	0.262	1.079
2	EDMA, 20mol%	0.618	2.261	0.171	0.627
3	TDMA, 20mol%	0.819	2.818	0.165	0.566
4	OD, 20mol%	0.472	2.044	0.255	1.102
5	DD, 20mol%	0.550	2.634	0.253	1.211
6	TD, 20mol%	0.722	3.099	0.278	1.194
7	DVB, 20mol%	0.854	2.993	0.201	0.704
8	DVN, 20mol%	0.947	3.523	0.228	0.848
9	PDMA, 20mol%	0.879	2.831	0.187	0.602

Conditions: 0.100 g 20mol% cross-linked polymer, 2.63 mL carbonate buffer solution, 0.063 -1.250 g fructose or glucose, 3 h, RT. \* - fit based on adsorption at low concentrations, since the highly viscous solution became impossible to filter at high concentrations.

A resonance corresponding to sp<sup>3</sup>-hybridized boron is present at a lower frequency (4 ppm) after pre-treatment with the phosphate buffer compared to pre-treatment with the carbonate buffer (5 ppm). The different shifts might be caused by molecular complexation of the phenylboronic acid with either phosphate or carbonate. Such interactions have been reported, although the contributions of such complexes are expected to be small due to competition with OH<sup>-</sup> anions under basic conditions (Fig. 14S).<sup>48</sup> The ratio of available sp<sup>3</sup> to sp<sup>2</sup> boron environments decreases in the following order: polymer treated with carbonate buffer, polymer dialysed after treatment with carbonate buffer, polymer treated with phosphate buffer, and polymer dialysed after treatment with phosphate buffer (Fig. 2a). Interestingly, the polymer pre-treated with the phosphate buffer exhibits a significantly higher fructose sorption capacity than the material pre-treated with carbonate buffer, even though the latter contains a higher fraction of sp<sup>3</sup>-hybridized boron atoms (Fig. 2b). Pre-treatment with the phosphate buffer results in a more pronounced swelling of the polymers. The swelling degrees after pre-treatment with phosphate or carbonate were 68 and 61%, respectively (Tab. 6S). The influence of the counter-anions on the swelling can be attributed to the polyelectrolyte swelling effect.<sup>49</sup> During pre-treatment, Na<sub>2</sub>CO<sub>3</sub> and NaHCO<sub>3</sub> as well as Na<sub>2</sub>HPO<sub>4</sub> and NaH<sub>2</sub>PO<sub>4</sub> are occluded by the polymer. During swelling, i.e. at pH 10, carbonate ions are present as a mixture of HCO<sub>3</sub><sup>-</sup> and CO<sub>3</sub><sup>2-</sup>, whereas all phosphate species are present as HPO<sub>4</sub><sup>2-</sup> anions. This leads to a higher repulsion between the doubly-charged hydrophosphate anions and the negatively charged boronate moieties, facilitating swelling. Dialysis of the polymers against water results in partial removal of the occluded phosphate and carbonate anions, causing a drop in swelling degree and adsorption capacity (Fig. 2b). In general, a positive effect of phosphates on the adsorption properties is observed. Therefore, all polymers were subsequently pre-treated with the phosphate buffer prior to adsorption experiments.

The pre-treated polymers contained predominantly sp<sup>2</sup> hybridized boron moieties along with a small share of the negatively charged sp<sup>3</sup> hybridized boronates (Fig. 2a). The portion of the negatively charged sp<sup>3</sup>-hybridized boron

moieties increases significantly upon fructose adsorption according to the solid-state <sup>11</sup>B NMR (Fig. 11S). We also tried to measure the zeta potential of the polymers before and after adsorption in order to detect negatively charged surface moieties upon adsorption. Unfortunately, the measurement failed due to insufficient dispersion of the particles in solution (for further details see p.14, SI).

After determining the effect of the polymer pre-treatment on the sorption behaviour, the influence of the cross-linker type and amount was evaluated. Polymers cross-linked with 5, 20, or 40 mol% DVB and EDMA were tested for fructose and glucose sorption. Maximum sorption capacities are listed in Tab. 2 (sorption isotherms, Fig. 15S-18S). The maximum sorption capacity decreases as the amount of cross-linker increases. This is a combined consequence of the accessibility of sorption-sites and the degree of polymer swelling. As expected, the higher the content of cross-linker, the lower the swelling degree of the polymer.<sup>50</sup> As noted for the influence of the pre-treatment conditions, more readily-swelling polymers exhibit higher adsorption capacities. Durability of the polymer, i.e. a capability of the polymer granules to maintain the shape under adsorption conditions, plays a crucial role for application. For example, the not cross-linked polymer dissolves completely in the fructose solution (Fig. 19S). Polymers with 5 mol% cross-linking give highly viscous liquids at high fructose concentrations, making it impossible to separate the polymer from the solution. In these cases, the Langmuir isotherm is based only on sorption values measured at low sugar concentration. This lowers the accuracy of the fit, such that the maximum sorption capacity exceeds 1 mol<sub>Fructose</sub>

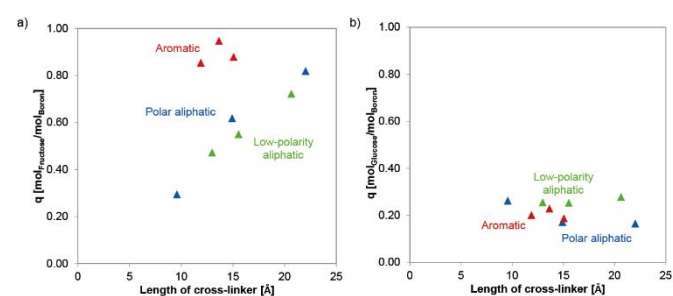


Figure 3: Dependence of the length of cross-linker on: a) the maximum fructose sorption capacity and b) the maximum glucose sorption capacity.



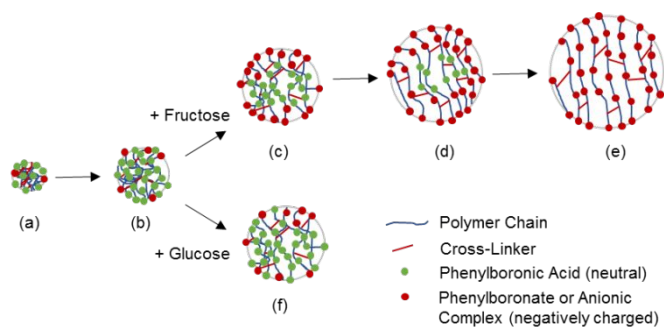


Figure 4: Schematic representation of the adsorption of fructose and glucose by phenylboronic acid-containing polymers.

$\text{mol}_B^{-1}$  (since complexation is based on a stoichiometric reaction between the boronate and the sugar, the theoretical maximum sorption capacity cannot exceed  $1 \text{ mol}_{\text{FRU}} \text{ mol}_B^{-1}$ ). A concentration of 20 mol% cross-linker was considered as a good compromise in maintaining sufficient polymer durability, while preserving a high sorption capacity.

To examine the influence of the nature of the cross-linker in more detail, polymers containing 20 mol% of different cross-linkers were tested for glucose and fructose sorption. Results are summarized in Tab. 3 (sorption isotherms, Fig. 20S-25S). Three series of cross-linkers as listed in Tab. 1 were tested, namely, polar aliphatic (DVS, EDMA, TDMA), low-polarity aliphatic (OD, DD, TD), and aromatic (DVB, PDMA, DVN) cross-linkers. In general, the fructose capacity increases with increasing length of the cross-linker, while the glucose capacity does not vary significantly for polymers with different cross-linkers (Fig. 3). Based on their commercial availability and a good compromise between high sorption capacity and sufficient durability, the cross-linked polymers containing 20 mol% DVB or EDMA were identified as most promising candidates and are therefore used in subsequent studies.

#### Adsorption: A General Discussion

The results for the adsorption of glucose and fructose can be interpreted using the scheme in Fig. 4.

Boron-containing polymers are non-porous. After pre-treatment with a basic solution, phenylboronic acid sites are partly converted to phenylboronates, i.e., they become negatively charged (a). Upon dispersion in carbonate buffer at pH 10, the polymers swell. Pre-treatment with a phosphate buffer facilitates swelling, owing to electrostatic repulsion between the phenylboronate sites and occluded  $\text{HPO}_4^{2-}$  anions. Complexation of phosphate by phenylboronate moieties (Fig. 14S) likely contributes to the improved swelling as well (b). Depending on the nature of the adsorbate, two scenarios are now possible. Fructose exhibits a high association constant with phenylboronates ( $K = 4370$ ).<sup>18</sup> Therefore, a high density of the fructose-phenylboronate complexes is expected (c). Since these complexes are negatively charged, further swelling takes place due to electrostatic repulsion between the polymer chains (d). During swelling, the polymer chains unfold and more phenylboronate moieties become available for adsorption. Eventually, the polymer is completely unfolded and all phenylboronate sites

Table 4: Swelling degree in the presence and absence of glucose and fructose for polymers cross-linked with 20 mol% DVB or 20 mol% EDMA, measured in the carbonate buffer solution.

Entry	Cross-linker	Swelling Degree [%]		
		Pure Buffer	In Presence of Fructose	In Presence of Glucose
1	20 mol% DVB	68	212	68
2	20 mol% EDMA	60	178	76

are accessible for adsorption (e). Such polymers exhibit their maximum capacity, corresponding to an equimolar fructose to boron loading. However, if the swelling is constrained, for example, by short cross-linkers or a high density of cross-linkers, some fraction of the phenylboronate sites remains inaccessible, i.e., case (d). Consequently, fructose adsorption is a self-sustaining process, due to repulsion between negatively charged complexes. This description explains why the maximum fructose adsorption capacity depends significantly on parameters that influence swelling, such as the pre-treatment method and the content and nature of the cross-linker.

The dependence of the fructose sorption capacity on the length of cross-linker is shown in Fig. 3a. Interestingly, the trends are the same for the polar and low-polarity aliphatic cross-linkers. Polymers containing aromatic cross-linkers exhibit higher sorption capacities for the same length, likely due to the more rigid structure compared to the more flexible aliphatic cross-linkers.<sup>51</sup> This trend is most obvious when comparing the maximum sorption capacities of the aromatic cross-linkers DVB, DVN, and PDMA. The maximum fructose capacity increases with the length of the aromatic cross-linker from DVB to DVN (Fig. 3a). However, a decrease in the maximum fructose capacity occurs for PDMA, although the cross-linker is longer. This decrease may be caused by the presence of polar groups in PDMA (see Tab. 1 for structures). This explanation is supported by the measurement of the swelling degree in presence of fructose: the PDMA-containing polymer swells significantly less compared to the polymers cross-linked with DVB and DVN (Tab.15S).

Adsorption of glucose is also depicted schematically in Fig. 4 (f). The association constant for complexation with phenyl-boronate ( $K = 110$ ) is significantly lower than for fructose.<sup>18</sup> As a result, the density of anionic complexes after adsorption is much lower. Thus, the polymers do not swell further, or swell insignificantly, upon interaction with glucose. The swelling degree in the presence of glucose and fructose was determined for the polymers cross-linked with 20 mol% DVB or 20 mol% EDMA (Tab. 4). The amount of adsorbed fructose and glucose is subtracted, thus the swelling degree is representative of the pure polymers.

These results confirm the insignificant swelling in the presence of glucose compared to pure buffer, whereas swelling is significantly enhanced in presence of fructose. Consequently, most of the phenylboronate moieties remain inaccessible to glucose. Since swelling does not take place during glucose adsorption, the sorption capacity for glucose is largely

independent of the pre-treatment method used, the cross-linker content, and the nature of the cross-linker. The maximum sorption capacities in dependence of the length of cross-linker are illustrated in Fig. 3b.

Fig. 4 also rationalizes the kinetics of adsorption. Homogeneous reactions between boronates and saccharides are typically complete within minutes.<sup>52</sup> However, it takes roughly 3 h and 90 min, respectively, for the adsorption of fructose and glucose to reach the equilibrium. In the first few minutes, rapid uptake of the sugar is observed, followed by slower adsorption (Fig. 12S-13S). Apparently, the rate of adsorption is not controlled solely by the complexation reaction but also by the swelling of the polymer. Equilibration is faster for glucose than for fructose, since the polymers swell much less during adsorption of glucose.

It is worth noting that the model proposed in Fig 4 does not consider changes in the electronic structure of boron caused by the varying nature of the cross-linker. Such changes cannot be completely excluded, since differences are present in the <sup>11</sup>B MAS NMR spectra of the materials (Fig. 11S).

### Structure of Sugar-Boronate Complexes

For a more in depth analysis, the composition of the sugar complexes formed upon adsorption was studied by *in situ* <sup>13</sup>C MAS-NMR.<sup>53</sup> To enhance the sensitivity and simplify the spectra, fructose and glucose were selectively <sup>13</sup>C-labelled at the anomeric carbons, which coordinate to the boronate in all complexation modes. For fructose, 2-<sup>13</sup>C-labelled fructose was used. Time-resolved spectra and assignments of signals to free fructose tautomers and fructose-boronate esters are shown in Fig. 5. Three fructose tautomers are identifiable in the spectra:  $\beta$ -fructopyranose ( $\beta$ -Frup),  $\beta$ -fructofuranose ( $\beta$ -Fruf), and  $\alpha$ -fructofuranose ( $\alpha$ -Fruf), at 97.8, 101.2, and 104.2 ppm, respectively. Concentrations of fructoketose (Fruk) and  $\alpha$ -fructopyranose ( $\alpha$ -Frup), are below the detection limit. Over time, the  $\beta$ -Frup signal declines in intensity while the concentrations of  $\beta$ -Fruf and  $\alpha$ -Fruf are almost unchanged. In addition to the fructose tautomers, five other resonances are present in the spectra. They are assigned to fructose-boronate esters, based on multiple literature reports.<sup>54, 55</sup> The signals of the sorbed species are not significantly broadened compared to those of the free fructose tautomers, suggesting that the fructose esters remain mobile. The most abundant species are three  $\beta$ -Frup monoboronates with signals at 114.7, 114.6, and

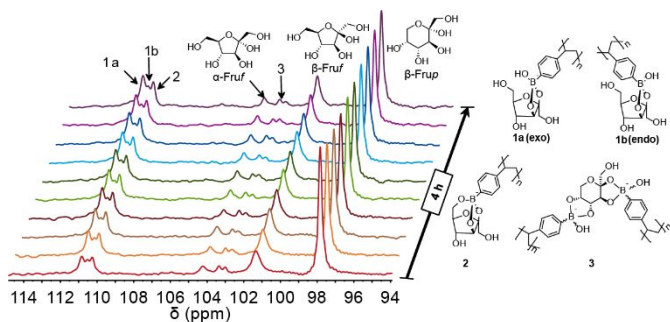


Figure 5: In situ array of direct polarization <sup>13</sup>C MAS-NMR spectra of fructose sorption on a 20 mol% DVB cross-linked phenylboronic acid polymer, showing three fructose tautomers and four fructose-boronate esters. Conditions: 80:20 v:v mixture of 0.5 M NaHCO<sub>3</sub>-buffer in D<sub>2</sub>O (pH adjusted to 10 with 4 M NaOH) and EtOH, RT.

Table 5: Fructose desorption efficiency in various acidic solutions, from polymers cross-linked with 20 mol% EDMA. Repetitive desorption (entries 9a-9c) was performed with the 20 mol% DVB cross-linked polymer.

Entry	Desorption Solution	DE [%]	Overall DE [%]
1	0.5 M H <sub>2</sub> SO <sub>4</sub> + 20 vol% EtOH <sup>a</sup>	89	
2	0.5 M H <sub>2</sub> SO <sub>4</sub> + 20 vol% EtOH	88	
3	0.5 M H <sub>2</sub> SO <sub>4</sub> +20 vol% EtOH <sup>b</sup>	91	
4	1 M Formic Acid	90	
5	1 M Acetic Acid	93	
6	1 M Acetic Acid+20 vol% EtOH	88	
7	1 M Acetic acid/acetate buffer	79	
8	CO <sub>2</sub> desorption, 30 bar, 50 °C	92	
9a	0.5 M H <sub>2</sub> SO <sub>4</sub> + 20 vol% EtOH	88	
9b	0.5 M H <sub>2</sub> SO <sub>4</sub> + 20 vol% EtOH <sup>c</sup>	9	97
9c	0.5 M H <sub>2</sub> SO <sub>4</sub> + 20 vol% EtOH <sup>d</sup>	2	99

Conditions: 100 mg polymer, 2.63 mL desorption solution, 4 h, RT. a: Measured using half the amount of desorption solution (1.32 mL), b: Measured using double the amount of desorption solution (5.25 mL), c: The polymer used in 9a was reused for a 2<sup>nd</sup> desorption, d: The polymer used in 9b was reused for a 3<sup>rd</sup> desorption.

113.4 ppm. The first two are the 2,3-exo and endo isomers (Fig. 5, 1a and 1b), respectively, whereas the last is a 2,3,6-tridentate complex (Fig. 5, 2). The three monoboronates form preferentially when the fructose-to-boron ratio is close to 1. Two additional signals, at 103.4 and 103.0 ppm, are most likely diboronate ester isomers.<sup>55</sup> Nicholls and Paul reported that diboronate esters can be formed at the 2,3- and 4,5-positions of the boat/twist conformers of  $\beta$ -Frup.<sup>56</sup> Two phenyl rings can have either endo or exo orientations, resulting in a total of four diastereomers (Fig. 5, 3). The structures of the four possible diboronate esters are similar, and thus the corresponding resonances are not well-resolved. Both mono- and di-boronate esters have been reported in the presence of organic diboronic acids.<sup>57</sup> Analysis of the different complexes formed with glucose, as well as time-resolved spectra showing the changes in concentration of free and sorbed fructose and glucose can be found in the SI (Fig. 26S-29S). According to the *in situ* NMR studies, the times required to establish equilibria between dissolved and adsorbed monosaccharides are 2 h for fructose and 1 h for glucose.

### Desorption

In addition to sugar adsorption, the subsequent desorption is important in the development of a separation process. Desorption is possible in acidic media, since the sugar complexes are unstable at low pH. High desorption efficiency was observed with 0.5 M aqueous H<sub>2</sub>SO<sub>4</sub> acid, which we previously used for extraction-assisted processes.<sup>35, 58-60</sup> Analogous to the adsorption procedure, 20 vol% EtOH was generally added to the desorption solutions to ensure polymer dispersion. Typical desorption experiments were performed at RT for 4 h. There is no significant influence of temperature (RT, 50, or 70 °C), and sugar concentration reaches a stable value after 4 h (Tab. 11S-12S).

Desorption efficiencies for various acidic solutions are high, in the range 79-93% (Tab. 5). The nature of the acidic solution

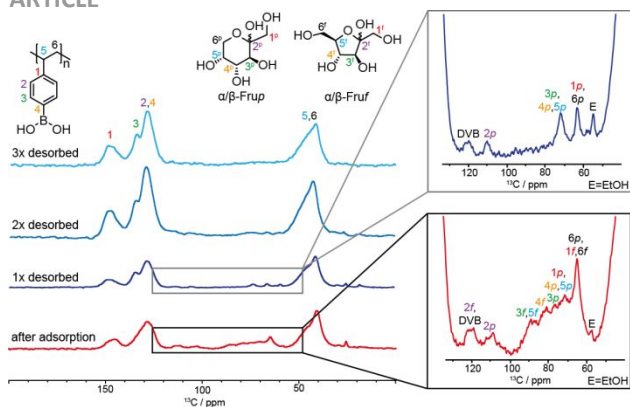


Figure 6:  $^{13}\text{C}$  CP/MAS NMR (24 KHz MAS, contact time 2.0 ms, 3072 scans) of the DVB-cross-linked polymer after adsorption and desorption. The recovered polymer was filtered and dried under high vacuum prior to analysis

has no notable influence on the desorption efficiency. An advantage of the organic acids (formic and acetic acid) is that both can be used without EtOH addition, while maintaining sufficient polymer dispersion (Tab. 5, entries 4 and 5). Fructose can be further desorbed into acidic solutions of smaller volume (Tab. 5, entries 1-3). This finding suggests a way to increase the final fructose concentration. Desorption into an acetate buffer at pH 4.75 was also efficient, indicating that even a slightly acidic pH is sufficient to induce boronate ester cleavage.

(Tab. 5, entry 7). Most importantly, efficient desorption was observed into a 80:20 v:v water:ethanol mixture in an autoclave pressurized with  $\text{CO}_2$  (Tab. 5, entry 8). The pH after desorption was 6.8. Utilization of  $\text{CO}_2$  presents an opportunity to improve the sustainability of the desorption process, yielding streams that are not contaminated with molecular acids. Desorption of glucose and saccharides from glucose-fructose mixtures with  $\text{CO}_2$  were also examined. These experiments showed feasibility of glucose desorption with  $\text{CO}_2$ , though a moderate desorption efficiency of 51% was observed (Tab.14S).

Tab. 5 shows that three consecutive desorption runs using  $\text{H}_2\text{SO}_4$  are necessary to completely desorb fructose (entries 9a-c). The progress of desorption was studied by  $^{13}\text{C}$  CP/MAS NMR. In addition to the resonances previously assigned to the polymer network, signals in the range 65 to 120 ppm are present after fructose adsorption. They are assigned to adsorbed fructopyranose ( $\alpha/\beta$ -Frup) and

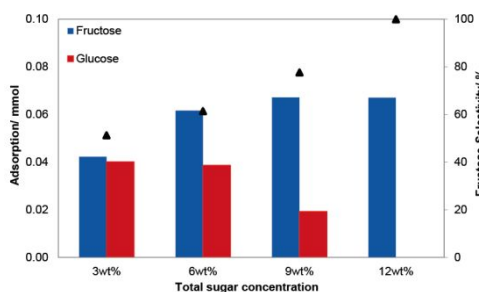


Figure 7: Competitive adsorption from a 70:30 mol%:mol% glucose:fructose model substrate mixture at varying total sugar concentrations. Conditions: 100 mg 20 mol% cross-linked EDMA polymer, 2.63 mL carbonate buffer solution, 3 h, RT.

fructofuranose ( $\alpha/\beta$ -Fruf, Fig. 6, inset 1). The lines are broad since multiple complexes with various configurations are present, as shown by *in situ*  $^{13}\text{C}$  MAS NMR (see section

Structure of Sugar-Boronate Complexes). Nevertheless, the ranges corresponding to resonances of furanose and pyranose complexes are recognizable (Fig. 6, insets 1+2). The specific assignments shown in both insets are supported by the work from Norrild and Eggert, who employed  $^1\text{J}_{\text{CC}}$  coupling constants to investigate *p*-tolylboronic acid-fructose complexes.<sup>55</sup> Interestingly, no signals corresponding to Fruf were observed after the first desorption, although resonances of Frup complexes are still visible (Fig. 6, inset 2). After three consecutive desorption runs, no resonances corresponding to boronate-saccharide complexes are present in the  $^{13}\text{C}$  CP/MAS NMR spectrum.

To examine the possibility of polymer recycling, consecutive adsorption-desorption cycles were performed under optimized conditions. Five repetitive adsorption-desorption cycles using 0.5M  $\text{H}_2\text{SO}_4$  and three recycling runs using pressurized  $\text{CO}_2$  for desorption were performed (Fig.30S and 31S). In each cycle, the polymer exhibited around 90% of the sorption capacity of the previous one. This result indicates a rather high durability of the polymer materials under adsorption and desorption conditions. Our current work focuses on investigation of long-term stability of the polymers in a continuous setup. This will enable further insight into fouling mechanisms of the polymers and required regeneration procedures. It is particularly noteworthy that no boron leaching was detected in the liquid phase upon recycling.

#### Adsorption-Assisted Isomerization

Finally, we explored the separation of glucose-fructose mixtures via polymer adsorption and the possibility of enhancing the fructose yield by combining separation with glucose-fructose isomerization. Competitive sorption from a model solution containing a 70:30 mol%:mol% glucose:fructose mixture demonstrates the feasibility for selective fructose recovery (Fig. 7). Adjusting the sugar to boron ratio has a major influence on selective recovery. At a low sugar to polymer ratio, free sorption sites remain available to bind glucose, whereas a high sugar to polymer ratio leads to saturation of the sorption sites with fructose.

First, the base-catalyzed isomerization of glucose to fructose was studied in the carbonate buffer, which was also used as a solvent for measuring sorption isotherms. The reaction is relatively fast at moderate temperatures, and a high selectivity towards fructose was observed. For example, a fructose yield of 24% was achieved at 25% glucose conversion after 1 h at 63 °C (Fig. 32S+33S). Barker et al. proposed that *in situ* adsorption of fructose on boron-containing polymers improves the fructose yield and facilitates product separation during glucose isomerization.<sup>39</sup> Using NaOH as the catalyst and a *p*-vinylphenylboronic acid polymer containing 5 mol% DVB, they reported a maximum fructose yield of 57% in the presence of the polymer. Therefore, we added a 20 mol% DVB cross-linked polymer to a reaction mixture containing glucose and carbonate buffer as catalyst.

However, the isomerization rate decreased significantly in the presence of the polymer, such that a maximum fructose yield of 27% at a glucose conversion of 58% was achieved only after

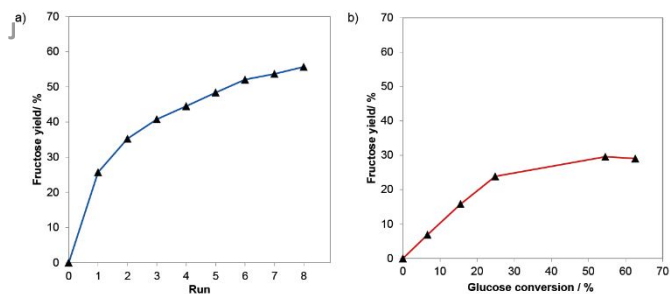


Figure 8: a) Adsorption-assisted isomerization: fructose yield after each of eight consecutive isomerization-separation cycles; b) dependence on glucose conversion of the fructose yield in glucose isomerization in the absence of polymer. Conditions: for glucose isomerization: 10 mL of 10 wt% glucose solution in carbonate buffer, 1 h at 63 °C; for adsorption: 6.57 mL isomerization solution added to 0.250 g polymer, 3 h at RT.

12 h. The reduction in reaction rate is consistent with glucose adsorption by the polymer, which lowers the effective glucose concentration in solution. Similar decreases in fructose yield and selectivity were observed during attempts to reproduce the experiments of Barker et al., and the reported yield of 57% was not achieved. In the presence of NaOH or carbonate buffer, the maximum yields of fructose were limited to 36% (at a fructose selectivity of 50%) and 27% (at a fructose selectivity of 46%), respectively. Furthermore, the polymers became colored, implying the adsorption of sugar degradation products (Fig. 40S).

Next, we studied the adsorption-assisted isomerization of glucose in consecutive isomerization and adsorption experiments. Glucose was first isomerized in the carbonate buffer, then the polymer was added to separate the fructose. The residual solution was used in a second isomerization cycle, after adding more glucose to restore the initial total sugar concentration. Eight consecutive isomerization-separation cycles were performed. The results summarized in Fig. 8 demonstrate the potential of the adsorption-assisted process. The maximum fructose yield almost doubled, from 29% in absence of the polymer to 56% for the adsorption-assisted reaction (compare Fig. 8a and b), comparable to the yield reported by Barker et al. Comparing the results to the previously reported extraction-assisted process,<sup>35</sup> a slight increase of fructose yield of 56% compared to 51% is obtained during the adsorption-assisted approach. Further advantages are the avoidance of an organic co-extraction solvent as well as the necessity of adding quaternary amines as counter-cations for the stabilization of the molecular boronate complex in the organic phase. The process is, therefore, highly promising. We are now working on improving the polymer material as well as the process design to improve the isolated fructose yield, i.e., optimizing the glucose isomerization conditions.

## Conclusions

This study described a method for fructose production via adsorption-assisted isomerization of glucose. Cross-linked poly(*p*-vinylphenylboronate) adsorbs fructose selectively from glucose isomerization reaction mixtures, making use of the preferential complexation of fructose by boronate moieties. In order to reach high fructose loading, high boron content is required. Our results show, however, that a compromise between boron content and durability is needed. High loadings

of ca. 1 mol<sub>Fructose</sub> mol<sub>B</sub><sup>-1</sup> can be achieved for polymers with low cross-linker content, but these materials become viscous substances under adsorption conditions. Polymers containing 20 mol% DVB or 20 mol% EDMA represent an attractive compromise, maintaining polymer durability and high sorption capacities of 0.854 and 0.618 mol<sub>Fructose</sub> mol<sub>B</sub><sup>-1</sup>, corresponding to 540 and 407 mg<sub>Fructose</sub> g<sub>polymer</sub><sup>-1</sup>, respectively. Moreover, these cross-linkers are commercially available. *Ex situ* and *in situ* MAS solid-state NMR provided molecular insight into the kinetics of sugar sorption as well as the nature of complex formation between sugar and boronate. These insights will help to further develop a highly efficient material for the separation of fructose from glucose. Desorption of fructose was possible using pressurized CO<sub>2</sub>, which represents a promising sustainable alternative to the use of non-volatile mineral acids. Overall, the adsorption-assisted approach is an attractive process with high potential for integration into value chains for the conversion of renewable feedstocks.

## Conflicts of interest

There are no conflicts to declare.

## Acknowledgements

We thank Simon Petring, Noah Avraham, Jens Heller, Heike Bergstein and Ines Bachmann-Remy for HPLC, CHN, ICP-OES and solution-state NMR analysis. We thank Christian Gierlich for computing the lengths of the cross-linkers. We thank DFG (Project 391305926) for financial support. G. S. acknowledges the German Federal Environmental Foundation (DBU) and the German Academic Exchange Service (DAAD) through its Thematic Network "ACalNet" funded by the German Federal Ministry of Education and Research (BMBF) for fellowship support. As part of the ACalNet project, G. S. and S. L. S. thank the U.S. National Science Foundation for support under Award CBET-1512228. L. Q. is supported by the U.S. Department of Energy, Office of Basic Energy Sciences, Division of Chemical Sciences, Geosciences, and Biosciences through the Ames Laboratory. The Ames Laboratory is operated for the U.S. Department of Energy by Iowa State University under Contract No. DE-AC02-07CH11358.

## Notes and references

1. S. E. Jacobsen and C. E. Wyman, *Twenty-First Symposium on Biotechnology for Fuels and Chemicals*, 2000, 81-96.
2. I. Delidovich, K. Leonhard and R. Palkovits, *Energy Environ. Sci.*, 2014, **7**, 2803-2830.
3. Y.-B. Huang and Y. Fu, *Green Chem.*, 2013, **15**, 1095-1111.
4. I. Delidovich and R. Palkovits, *ChemSusChem*, 2016.
5. L. M. Hanover and J. S. White, *Am. J. Clin. Nutr.*, 1993, **58**, 724S-732S.
6. J. M. Carraher, C. N. Fleitman and J.-P. Tessonnier, *ACS Catal.*, 2015, **5**, 3162-3173.
7. Y. B. Tewari, *Biotechnol. Appl. Biochem.*, 1990, **23**, 187-203.

8. A. A. Rosatella, S. P. Simeonov, R. F. Frade and C. A. Afonso, *Green Chem.*, 2011, **13**, 754-793.
9. J. J. Bozell and G. R. Petersen, *Green Chem.*, 2010, **12**, 539-554.
10. D. W. Rackemann and W. O. Doherty, *Biofuel Bioprod. Biorefin.*, 2011, **5**, 198-214.
11. K.-U. Klatt, F. Hanisch and G. Dünnebier, *J. Process Control*, 2002, **12**, 203-219.
12. H. Li, S. Yang, S. Saravanamurugan and A. Riisager, *ACS Catal.*, 2017, **7**, 3010-3029.
13. S. Ramaswamy, H.-J. Huang and B. V. Ramarao, *Separation and purification technologies in biorefineries*, John Wiley & Sons, 2013.
14. J. A. Vente, H. Bosch, A. B. de Haan and P. J. Bussmann, *Adsorpt. Sci. Technol.*, 2006, **24**, 771-780.
15. G. Springsteen and B. Wang, *Chem. Commun.*, 2001, 1608-1609.
16. G. Springsteen and B. Wang, *Tetrahedron*, 2002, **58**, 5291-5300.
17. J. Yan, G. Springsteen, S. Deeter and B. Wang, *Tetrahedron*, 2004, **60**, 11205-11209.
18. J. P. Lorand and J. O. Edwards, *J. Org. Chem.*, 1959, **24**, 769-774.
19. S. Shinkai, K. Tsukagoshi, Y. Ishikawa and T. Kunitake, *J. Chem. Soc., Chem. Commun.*, 1991, 1039-1041.
20. D. C. Klenk, G. T. Hermanson, R. I. Krohn, E. K. Fujimoto, A. K. Mallia, P. Smith, J. England, H. Wiedmeyer, R. Little and D. Goldstein, *Clin. Chem.*, 1982, **28**, 2088-2094.
21. T. R. Jackson, J. S. Springall, D. Rogalle, N. Masumoto, H. Ching Li, F. D'Hooge, S. P. Perera, T. A. Jenkins, T. D. James and J. S. Fossey, *Electrophoresis*, 2008, **29**, 4185-4191.
22. Y.-H. Zhao and D. F. Shantz, *Langmuir*, 2011, **27**, 14554-14562.
23. T. C. Brennan, S. Datta, H. W. Blanch, B. A. Simmons and B. M. Holmes, *Bioenergy Res.*, 2010, **3**, 123-133.
24. J. Shi, J. M. Gladden, N. Sathitsuksanoh, P. Kambam, L. Sandoval, D. Mitra, S. Zhang, A. George, S. W. Singer and B. A. Simmons, *Green Chem.*, 2013, **15**, 2579-2589.
25. G. Griffin, *Sep. Sci. Technol.*, 2005, **40**, 2337-2351.
26. B. R. Caes, R. E. Teixeira, K. G. Knapp and R. T. Raines, *ACS Sustain. Chem. Eng.*, 2015, **3**, 2591-2605.
27. B. Li, S. Varanasi and P. Relue, *Green Chem.*, 2013, **15**, 2149-2157.
28. G. John Griffin and L. Shu, *J. Chem. Technol. Biotechnol.*, 2004, **79**, 505-511.
29. B. Li, P. Relue and S. Varanasi, *Green Chem.*, 2012, **14**, 2436-2444.
30. H. A. Aziz, A. Kamaruddin and M. A. Bakar, *Sep. Purif. Technol.*, 2008, **60**, 190-197.
31. S. Alipour, *Green Chem.*, 2016, **18**, 4990-4998.
32. S. Alipour and H. Omidvarborna, *RSC Adv.*, 2016, **6**, 111616-111621.
33. R. R. Broekhuis, S. Lynn and C. J. King, *Ind. Eng. Chem. Res.*, 1996, **35**, 1206-1214.
34. S. S. Gori, M. V. R. Raju, D. A. Fonseca, J. Satyavolu, C. T. Burns and M. H. Nantz, *ACS Sustain. Chem. Eng.*, 2015, **3**, 2452-2457.
35. I. Delidovich and R. Palkovits, *Green Chem.*, 2016, **18**, 5822-5830.
36. P. J. Duggan, *Aust. J. Chem.*, 2004, **57**, 291-299.
37. S. J. Gardiner, B. D. Smith, P. J. Duggan, M. J. Karpa and G. J. Griffin, *Tetrahedron*, 1999, **55**, 2857-2864.
38. M. Di Luccio, B. Smith, T. Kida, C. Borges and T. Alves, *J. Membr. Sci.*, 2000, **174**, 217-224.
39. S. Barker, B. Hatt, P. Somers and R. Woodbury, *Carbohydr. Res.*, 1973, **26**, 55-64.
40. A. K. Hoffmann and W. Thomas, *J. Am. Chem. Soc.*, 1959, **81**, 580-582.
41. R. Boulos and J. Feutrill, *U.S. Patent Application No. 15/748,514*, 2018.
42. V. Davankov, M. Tsyurupa and S. Rogozhin, *Angew. Makromolek. Chem.*, 1976, **53**, 19-27.
43. *Matlab 2018a and Global Optimization Toolbox*, The MathWorks, Inc.: Natick Massachusetts United States, 2018.
44. J. W. Wackerly and J. F. Dunne, *J. Chem. Educ.*, 2017, **94**, 1790-1793.
45. H. Nöth and B. Wrackmeyer, *Nuclear magnetic resonance spectroscopy of boron compounds*, Springer Science & Business Media, 2012.
46. J. A. Peters, *Coord. Chem. Rev.*, 2014, **268**, 1-22.
47. R. M. C. Dawson, D. C. Elliott, W. H. Elliott and K. M. Jones, *Data for biochemical research*, Clarendon Press, Oxford, UK, 1986.
48. L. Bosch, T. Fyles and T. D. James, *Tetrahedron*, 2004, **60**, 11175-11190.
49. S. T. Dubas and J. B. Schlenoff, *Langmuir*, 2001, **17**, 7725-7727.
50. G. Wulff, J. Vietmeier and H. G. Poll, *Angew. Makromolek. Chem.*, 1987, **188**, 731-740.
51. M. Takayanagi, T. Ogata, M. Morikawa and T. Kai, *J. Macromol. Sci. B*, 1980, **17**, 591-615.
52. W. A. Marinaro, R. Prankerd, K. Kinnari and V. J. Stella, *J. Pharm. Sci.*, 2015, **104**, 1399-1408.
53. L. Qi, R. Alamillo, W. A. Elliott, A. Andersen, D. W. Hoyt, E. D. Walter, K. S. Han, N. M. Washton, R. M. Rioux and J. A. Dumesic, *ACS Catal.*, 2017, **7**, 3489-3500.
54. R. van den Berg, J. A. Peters and H. van Bekkum, *Carbohydr. Res.*, 1994, **253**, 1-12.
55. J. C. Norrild and H. Eggert, *J. Chem. Soc., Perkin Trans. 2*, 1996, 2583-2588.
56. M. P. Nicholls and P. K. Paul, *Org. Biomol. Chem.*, 2004, **2**, 1434-1441.
57. S. P. Draffin, P. J. Duggan, S. A. Duggan and J. C. Norrild, *Tetrahedron*, 2003, **59**, 9075-9082.
58. P. Drabo, T. Tiso, B. Heyman, E. Sarikaya, P. Gaspar, J. Förster, J. Büchs, L. M. Blank and I. Delidovich, *ChemSusChem*, 2017, **10**, 3252-3259.
59. I. Delidovich, M. S. Gyngazova, N. Sánchez-Bastardo, J. P. Wohland, C. Hoppe and P. Drabo, *Green Chem.*, 2018, **20**, 724-734.
60. N. Sánchez-Bastardo, I. Delidovich and E. Alonso, *ACS Sustain. Chem. Eng.*, 2018, **6**, 11930-11938.

## Structure-performance correlations of cross-linked boronic acid polymers as adsorbents for recovery of fructose from glucose-fructose mixtures

Guido Schroer,<sup>a</sup> Jeff Deischter,<sup>a</sup> Tobias Zensen,<sup>a</sup> Jan Kraus,<sup>b</sup> Ann-Christin Pöppler,<sup>b</sup> Long Qi,<sup>c</sup> Susannah Scott,<sup>d,e</sup> and Irina Delidovich<sup>a,\*</sup>

This article addresses the utilization of cross-linked phenylboronic-acid polymers for fructose separation from glucose-fructose mixtures focusing particularly on structure-sorption relationships.

